

On the evolution of cooling cores in X-ray galaxy clusters

S. Etti¹, F. Brighenti²

¹ INAF, Osservatorio Astronomico di Bologna, via Ranzani 1, I-40127 Bologna, Italy (stefano.ettori@oabo.inaf.it)

² Dipartimento di Astronomia, Università di Bologna, via Ranzani 1, I-40127 Bologna, Italy (fabrizio.brighenti@unibo.it)

ABSTRACT

To define a framework for the formation and evolution of the cooling cores in X-ray galaxy clusters, we study how the physical properties change as function of the cosmic time in the inner regions of a 4 keV and 8 keV galaxy cluster under the action of radiative cooling and gravity only. The cooling radius, R_{cool} , defined as the radius at which the cooling time equals the Universe age at given redshift, evolves from $\sim 0.01R_{200}$ at $z > 2$, where the structures begin their evolution, to $\sim 0.05R_{200}$ at $z = 0$. The values measured at $0.01R_{200}$ show an increase of about 15–20 per cent per Gyr in the gas density and surface brightness and a decrease with a mean rate of 10 per cent per Gyr in the gas temperature. The emission-weighted temperature diminishes by about 25 per cent and the bolometric X-ray luminosity rises by a factor ~ 2 after 10 Gyrs when all the cluster emission is considered in the computation. On the contrary, when the core region within $0.15R_{500}$ is excluded, the gas temperature value does not change and the X-ray luminosity varies by 10 – 20 per cent only. The cooling time and gas entropy radial profiles are well represented by power-law functions, $t_{\text{cool}} = t_0 + t_{0.01}(r/0.01R_{200})^\gamma$ and $K = K_0 + K_{0.1}(r/0.1R_{200})^\alpha$, with t_0 and K_0 that decrease with time from 13.4 Gyrs and 270 keV cm² in the hot system (8.6 Gyr and 120 keV cm² in the cool one) and reach zero after about 8 (3) Gyrs. The slopes vary slightly with the age, with $\gamma \approx 1.3$ and $\alpha \approx 1.1$. The behaviour of the inner slopes of the gas temperature and density profiles are the most sensitive and unambiguous tracers of an evolving cooling core. Their values after 10 Gyrs of radiative losses, $T_{\text{gas}} \propto r^{0.4}$ and $n_{\text{gas}} \propto r^{-1.2}$, are remarkably in agreement with the observational constraints available for nearby X-ray luminous cooling core clusters. Because our simulations do not consider any AGN heating, they imply that the feedback process does not greatly alter the gas density and temperature profiles as generated by radiative cooling alone.

Key words: X-ray: galaxies – galaxies: clusters: general

1 INTRODUCTION

The hot plasma in groups and clusters of galaxies during the hierarchical formation of dark matter halos cools by bremsstrahlung and line emission regulated by n_{gas}^2 . The action of the cooling is thus more effective in the central regions at higher density, with a twofold effect of decreasing the temperature and rising the density moving inwards. In recent years, the new generation of X-ray telescopes like *Chandra* and *XMM-Newton* has been able to spatially resolve the emission from the central regions characterizing the physical properties of the X-ray emitting plasma. These observations have revealed that the cooling is not the only mechanism that is responsible for the energetic of the central gas. Still-debated feedback processes have to play a relevant role in its thermal evolution (e.g. Peterson & Fabian 2006).

A further unknown property is how a cool core evolve with cosmic time. Bauer et al. (2005) find that cool cores appear to be common at redshift 0.15 – 0.4, even though there is mounting evidence that they are less numerous and/or prominent at higher redshift (Etti et al. 2004, Vikhlinin et al. 2006b, Santos et al. 2008). In the present work, we try to address this issue from a theoretical

point of view, just considering how a plasma in hydrostatic equilibrium with a NFW potential with global quantities consistent with present-day observational constraints, changes its physical properties as function of the cosmic time under the action of the radiative cooling only. This simple model allows to define a framework in which we can make zero-th order predictions on the formation, evolution and fate of a cooling core in X-ray groups and clusters of galaxies, taking into consideration that any deviation from these expectations has to refer to the variety of the heating mechanisms that can affect the energy budget of the structure.

The paper is organized as follow: after the presentation of the numerical model adopted to describe the X-ray emitting plasma in hydrostatic equilibrium in a dark matter potential, we discuss in Section 3 the evolution in the observable properties of a cooling core like the cooling radius, R_{cool} , the cooling time, t_{cool} , the gas temperature, density, entropy and surface brightness profiles. We present the models that reproduce the radial behaviour and the fitting parameters that are more strongly correlated with the age of the structure, being older structures the ones with the lower cooling time at given radius. A comparison with the observational constraints is also discussed in Section 3.3. Finally, our results and

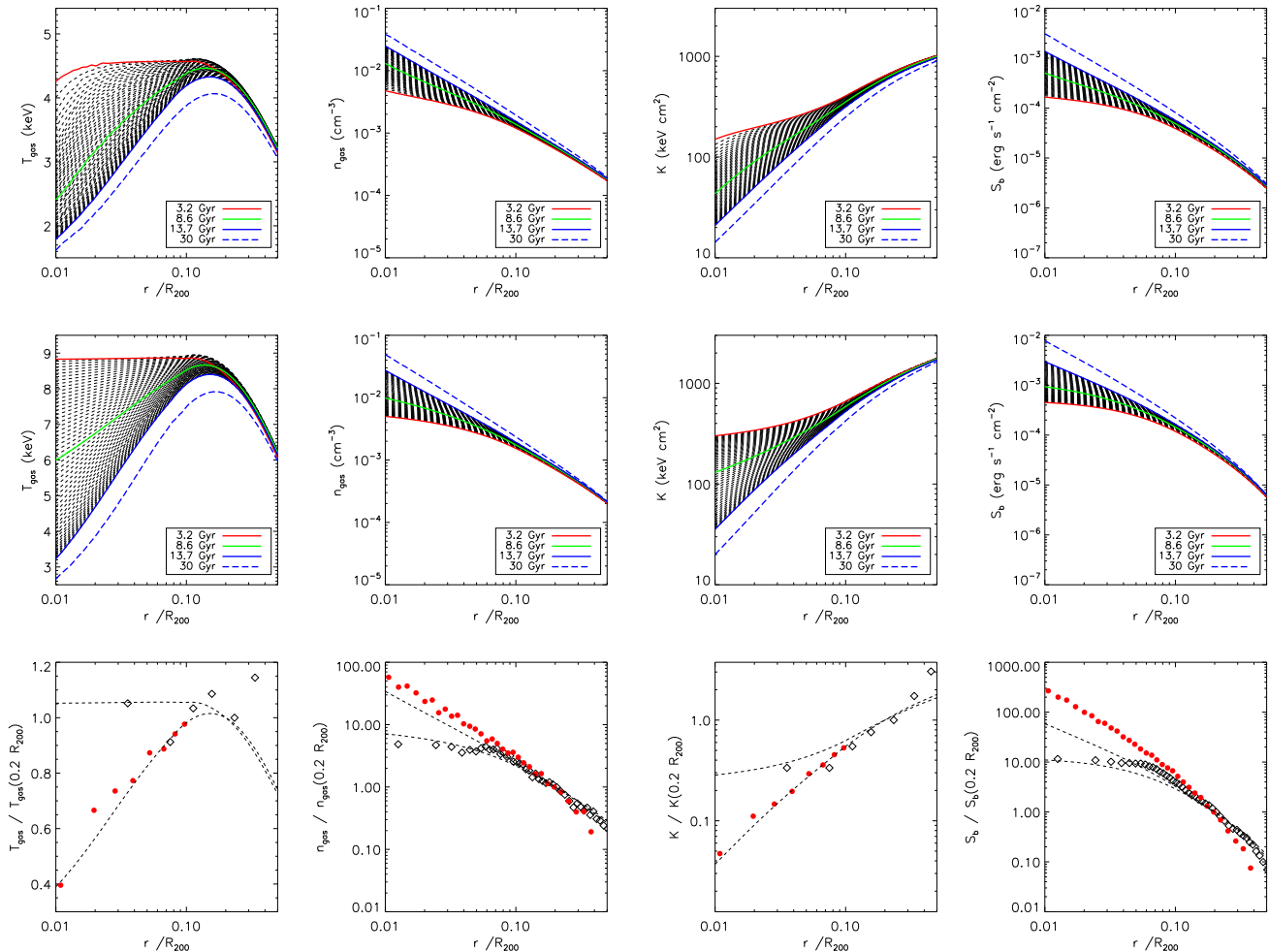


Figure 1. Evolution of the gas temperature, density, entropy and surface brightness profiles from redshift 2.1 ($t = 3.2$ Gyr) up to the present time ($t = 13.7$ Gyr) for the “4 keV” cluster (*upper panels*) and the “8 keV” cluster (*middle panels*). For the latter case, we also show, for pedagogical reasons, the expected profiles at $t = 30$ Gyr, i.e. at about 16 Gyr in the future. In the *lower panels*, we show the profiles renormalised at the value at $0.2R_{200}$ for a cool-core (A1795 and A1835; red dots) and a non-cool-core (A665; black diamonds) cluster. The dashed lines show the simulated profiles at the beginning and end of the evolution.

discussion are summarized in Section 4. Throughout this work we adopt the following cosmological parameters: $H_0 = 70 \text{ km s}^{-1} \text{ Mpc}^{-1}$, $\Omega_m = 1 - \Omega_\Lambda = 0.27$, that implies a present age of the Universe of 13.8 Gyr.

2 THE NUMERICAL SIMULATIONS

The calculations presented below are based on the time dependent 1D hydrodynamical equations described in Brighenti & Mathews (2002) with the heating, conduction and convection terms set to zero. The cooling function is modelled according to Sutherland & Dopita (1993), using a metallicity dependent fitting formula. Here the abundance is set to $0.4 Z_\odot$.

To solve the equations we use a modified version of the public code ZEUS2D (Stone & Norman 1992). We adopt spherical coordinates, and the grid extends from $r = 0$ to $r_{\text{max}} \sim 10 \text{ Mpc}$ in 360 zones. The grid size is $\Delta r = 0.5 \text{ kpc}$ at the center and slowly increases toward large radii.

Our simulations start with gas in hydrodynamical equilibrium

in a potential well formed by a NFW dark matter halo (Navarro, Frenk & White 1996) and a de Vaucouleurs profile representing the central galaxy. Although not crucial, the presence of the galaxy and the associated mass and energy sources have second order effects on the ICM evolution. The reader is referred to Brighenti & Mathews (2002) for details about stellar mass return and SNIa heating due to the central galaxy. For the sake of simplicity, the gravitational potential is kept constant in time. Neglecting the cosmic growth of the dark halo has some influence in the inner structure of clusters, although halos grow mostly inside-out and the gravitational potential in the core region changes little with time during the smooth accretion phase between major mergings (Zhao et al., 2003, Salvador-Solé et al. 2007, Li et al. 2007). The initial temperature profile follows the one described in Vikhlinin et al. (2006a) for $r \geq 0.15 R_{500}$ (where R_{500} is defined below):

$$T(r) = 1.216T_x \frac{(x/0.045)^{1.9} + 0.45}{(x/0.045)^{1.9} + 1} \frac{1}{[1 + (x/0.6)^2]^{0.45}}$$

while is isothermal $T(r) = T(0.15 R_{500})$ for $r < 0.15 R_{500}$. Here T_x is the global (spectroscopic) temperature, calculated ac-

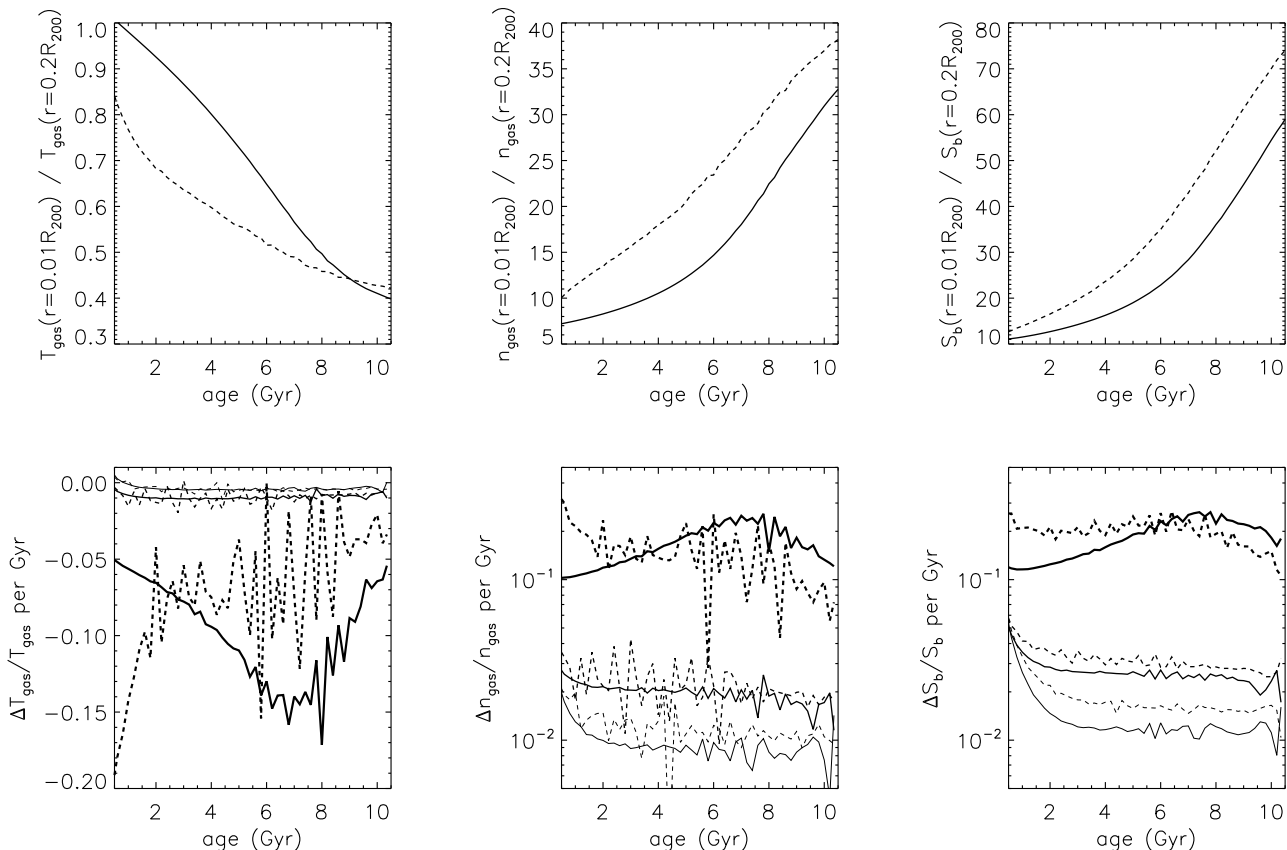


Figure 2. Upper panels Ratios between the gas temperature (left), density (middle) and surface brightness (right) estimated at $0.2R_{200}$ and $0.01R_{200}$ versus the age of the hot (solid line) and cool (dashed line) object. **Lower panels** Relative variation per Gyr as function of the structure’s age in the hot (solid line) and cold (dashed line) object. The relative changes are estimated at 0.01, 0.1, $0.2R_{200}$ from thickest to thinnest lines, respectively.

cording to the observational mass-temperature relation by Arnaud et al. (2005) (see also Shimizu et al. 2003). The adopted initial temperature profile should represent a reasonable initial condition to study the radiative evolution of the cluster cores. The outer region ($r \geq 0.15 R_{500}$) is not greatly influenced by radiative cooling and thus we decided to set it to agree with current observations. In section 3.3 we briefly discuss how the results depend on the choice of the initial conditions.

We present results for two cluster models. The “hot”, massive cluster has a virial dark matter mass $M_{\text{DM,hot}} = 1.3 \times 10^{15} M_{\odot}$, while the “cold” object has $M_{\text{DM,cold}} = 4.1 \times 10^{14} M_{\odot}$. The concentration of the dark matter halo is calculated by fitting the $c - M$ relation given in Bullock et al. (2001): $c = 8.35 (M_{\text{DM}}/10^{14} M_{\odot})^{-0.911}$. The central galaxy is the same for the two models and has a stellar density profile following the approximation for a deprojected de Vaucouleurs law, given by Mellier & Mathez (1987). The total mass of the galaxy is assumed to be $M_* = 5.8 \times 10^{11} M_{\odot}$ and the effective radius is $R_e = 8.5$ kpc. These numbers are typical for giant elliptical galaxies. The initial gas temperature are $T_0 = 7.67$ keV and $T_0 = 4.0$ keV for the hot cluster and the cold cluster respectively. The initial central gas density is set by the requirement that the baryon fraction at the virial radius is similar to the cosmic one, i.e. we require $f_b(R_{\text{vir}}) = 0.16$ (e.g. Spergel et al. 2007). This results in $\rho_0 = 2.26 \times 10^{-26} \text{ g cm}^{-3}$ for the cold cluster and $\rho_0 = 1.82 \times 10^{-26} \text{ g cm}^{-3}$ for the hot cluster. The central cooling time, defined as

$t_{\text{cool}} = 2.5k\rho T / \mu m_p / n_e n_H \Lambda(T)$, is ~ 3.4 Gyr (cold cluster) and ~ 8.5 Gyr (hot cluster).

In order to better compare the modelled temperature with observations we present results for both the emission weighted temperature $T_{ew}(r)$ and the “spectroscopic-like” temperature $T_{sp}(r)$ defined in Mazzotta et al. (2004). T_{ew} is calculated in the usual way as the line of sight integral $T_{ew} = \int T \epsilon dl / \int \epsilon dl$, where ϵ is the (bolometric) gas emissivity, while $T_{sp} = \int T (n^2 T^{-0.75}) dl / \int n^2 T^{-0.75} dl$. According to Mazzotta et al. (2004) T_{sp} is a good approximation to the temperature measured with *Chandra* and *XMM* when the thermal structure of the ICM is complex. By performing the integral along the line of sight at any radius, we calculate a projected temperature profile which can be directly contrasted with the observed ones. The global temperature in a given region (i.e. $0 < r < R_{500}$) is then calculated with a similar weighted average: $T_{sp}(0 - R_{500}) = \int_0^{R_{500}} T_{sp}(r) (n^2 T^{-0.75}) 4\pi r^2 dr / \int_0^{R_{500}} n^2 T^{-0.75} 4\pi r^2 dr$.

In the following we will normalize the radial distances by R_{200} or R_{500} , the radii at which the overdensity is 200 or 500 respectively. For our two models we have: $R_{200} = 1.41$ Mpc, $R_{500} = 0.93$ Mpc (cold cluster) and $R_{200} = 2.05$ Mpc, $R_{500} = 1.34$ Mpc (hot cluster).

3 THE EVOLUTION OF THE RADIAL PROFILES

The calculations described here are similar to the unheated flow presented in Brighenti & Mathews (2003), where the reader may find a description of the thermal evolution of the flow. Recently, Guo & Oh (2007) have also discussed simulations of the ICM in a $T \sim 4$ keV cluster. The results of our calculations are in qualitative agreement with those in the two aforementioned papers. As the gas cools in the central region, it slowly flows inward to approximately preserve equilibrium. A positive temperature gradient develops and the density profile steepens. At the end of the simulations the temperature profile agrees nicely with typical observed cool core clusters (Figure 1), while the computed density is somewhat flatter. This can be understood with the long initial central cooling time (see above), which makes the “radiative age” of our models rather young, even after ~ 10 Gyr. After about one cooling time the gas in the centre cools to very low temperature, this is the onset of the so-called cooling catastrophe. The mass cooling rate grows with time, reaching an approximate steady-state after few cooling times (see Brighenti & Mathews 2003, 2006). In the calculations presented here the mass cooling rates are still increasing at the end of the simulations, due to the rather long initial cooling times. At $t = 13.7$ Gyr we find $\dot{M}_{\text{cool}} \approx 70$ (40) M_{\odot}/yr for the hot (cold) cluster. A total mass of $\sim 1.1 \times 10^{11} M_{\odot}$ and $\sim 1.3 \times 10^{11} M_{\odot}$ is cooled below X-ray temperature in the hot and cold cluster respectively. This is at odd with observations, which show tight constraints on the cooling rate (e.g. Peterson & Fabian 2006) – a blatant manifestation of the cooling flow problem. We do not attempt to solve this problem here (see McNamara & Nulsen 2007 for a recent review on this subject). Rather, we are interested in the formation of the cool core following the assembly of the cluster or the last major merging. The way in which the heating necessary to halt radiative cooling influences the density and temperature profiles is not well known. Here we take the position that the average thermal structure of the ICM is not greatly affected by the heating process. This appears justified by the reasonable agreement shown in Figure 1 below between observed and simulated, purely radiative temperature profile (see Brighenti & Mathews 2006 and Guo & Oh 2007 for models in which the variables profiles are not significantly modified by jet heating). Following this assumption we neglect the gravity from the unrealistic accumulation of cold gas in the centre of our models, which would generate a strong temperature peak (Brighenti & Mathews 2000).

The radial profiles of the gas temperature, density and surface brightness are obtained at temporal steps of 0.2 Gyr starting from the cosmic time of 3 Gyr, corresponding to $z = 2.11$ for the assumed cosmology, and reaching $z = 0$ after 10.7 Gyr. These profiles are plotted in Fig. 1. When we refer to the age of the structure, we mean the cosmic time at which the physical quantity is observed *minus* the cosmic time at which the structure started its evolution, i.e. 3 Gyr. In the same figure, we present the profiles normalized at the values observed at $0.2R_{200}$ in a cool-core (A1835 from Morandi & Ettori 2007 and A1795, for the inner regions, from Ettori et al. 2001) and a non-cool-core (A665, Morandi & Ettori 2007) massive cluster. The profiles follow the predicted behaviour in particular of the gas density and surface brightness distribution. Larger deviations are observed in the temperature profile that depend strongly on the reference global value adopted to normalize the profile.

We present in Fig. 2 the relative variation of the temperature, density and surface brightness as function of the age of the objects, both as ratios between the quantities estimated at fixed fractions

of R_{200} (i.e. $0.01R_{200}$, that lies well within the cluster core, and $0.2R_{200}$, radius at which the cooling is not effective anymore) and as relative changes per Gyr at $0.01, 0.1, 0.2R_{200}$. The expected behaviour is confirmed for all the quantities under exam with the added value that we are now in condition to quantify the magnitude of the variations.

The temperature decreases rapidly at first, with relative changes between 5 and 20 per cent per Gyr when measured at $0.01R_{200}$. After ~ 7 Gyr the temperature profile of the two objects reaches a quasi-steady state. This results in a ratio $T(r = 0.01R_{200})/T(r = 0.2R_{200})$ equals to ~ 0.4 after 10 Gyr of pure cooling flow evolution.

The gas density rises at a rate of about 15-20 per cent per Gyr when measured at $0.01R_{200}$ and of 1 per cent when the increase is evaluated at $0.2R_{200}$. After 10 Gyr, the ratio between these values is about 35, a factor $\sim 4 - 5$ larger than the ratio measured at the beginning of the formation of the cooling core.

The surface brightness, roughly proportional to the integral along the line of sight of the squared density, amplifies the variations observed in the density profile and is observed to increase with a mean rate of 16 and 1 per cent per Gyr at 0.01 and $0.2R_{200}$, respectively, with a ratio that rises from 10 to 60–70 at the present time, both in cool and hot systems.

3.1 Modelization of the radial profiles

To characterize the evolution of the cooling core, we consider the results of the modelization of the radial profiles of the X-ray quantities as function of the cosmic time.

We model the gas temperature, density and surface brightness profiles shown in Figure 1 with analytic formulae commonly used in the literature, which provide a good description of both observed and simulated profiles:

$$\begin{aligned} T_{\text{gas}} &= a_2 \frac{1 + x_0^{a_3}}{(1 + x_1^2)^{a_4}} \\ n_{\text{gas}} &= b_2 x_0^{-b_3} (1 + x_1^2)^{-1.5b_4} \\ S_b &= c_2 x_0^{-c_3} (1 + x_1^2)^{0.5-3c_4} \end{aligned} \quad (1)$$

where x_0 and x_1 are the radius rescaled for the corresponding scale radius (e.g., $x_0 = r/a_0$ or r/b_0 or r/c_0). To avoid some degeneracy among the parameters describing the temperature profile, we fix the inner scale radius, a_0 , to $0.05R_{200}$. A least squares fit is then performed between $0.01R_{200}$ and $0.5R_{200}$, where the numerical simulations provide more robust results, propagating a relative error comparable to the observational constraints (without any significant change in the best-fit results, we have adopted errors in the range of few per cent on the surface brightness, 5-15 per cent on the gas density, 10-20 per cent on the temperature values).

In general, single power-laws provides a good description of these profiles over partial sections of the radial profile, suggesting that cooling alone is not able to reproduce an emission shaped with an inner, well-defined core. For instance, while a single β -model well reproduces the outskirts of the gas density and surface brightness profile, a second inner component, either a power-law as in equation. 1 or an additive β -model, is characterized by very small core radii, of the order of the lower end of the investigated radial range of $0.01R_{200}$, and a factor between 5 and 10 lower than the external core radius.

A power-law + constant describes properly the gas entropy profile, $K = T_{\text{gas}}/n_{\text{gas}}^{2/3}$,

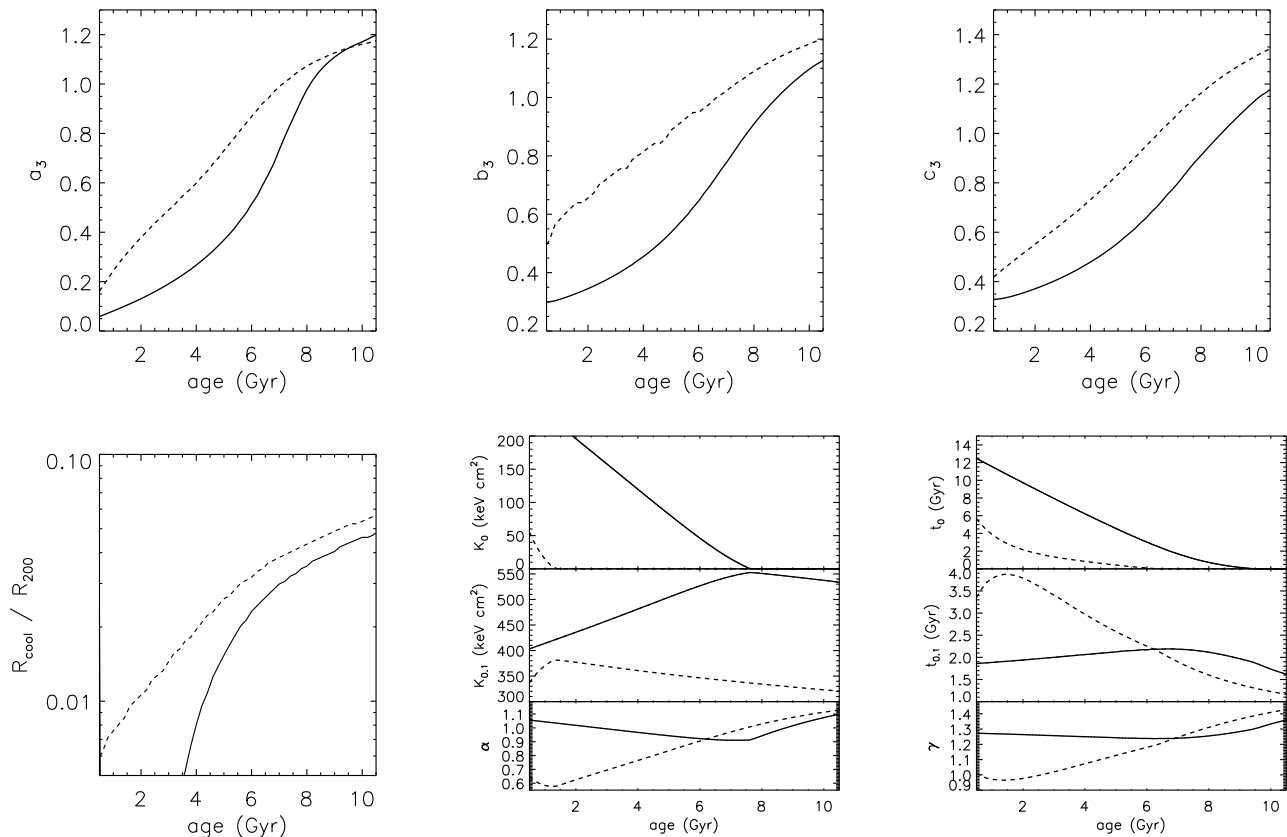


Figure 3. Properties of the cool cores as function of the clusters age for the “4 keV” (*dashed line*) and the “8 keV” object (*solid line*). (**Upper panels**) Evolution with the cosmic time of few significant best-fit parameters in Eq. 1 (see text in Sect 3.2). (**Lower panels**) Evolution of the cooling radius defined as the radius at which the cooling time equals the Universe age at given redshift (*left*); distribution of the best-fit parameters of the entropy profile (*middle*; cf. Eq. 2) and of the cooling time profile (*right*; see Eq. 3).

$$K = K_0 + K_{0.1} \left(\frac{r}{0.1R_{200}} \right)^\alpha, \quad (2)$$

and the cooling time profile,

$$t_{\text{cool}} = t_0 + t_{0.01} \left(\frac{r}{0.01R_{200}} \right)^\gamma, \quad (3)$$

over the radial range $0.01 - 0.1R_{200}$, as we discuss in the following subsection.

3.2 Best-fit parameters and age of the structure

We find that all the parameters that describe the structure of the cluster core are strongly correlated with its age. When a single power-law is fitted in the inner regions, the slope in the gas temperature profile starts from a value of zero (due to the initial isothermal assumption) and reaches ~ 0.40 at $z = 0$ in the cool and hot system, respectively, under the action of the increasing radiative cooling. Once equation 1 with $a_0 = 0.05R_{200}$ is fitted, the steepening of the inner gradient is well represented by the parameter a_3 , that rises from 0.1 up to 1.2 as the cooling core evolves (see Fig. 3). At the same time, a_1 decreases significantly with the age from $0.4 - 0.5R_{200}$ to values around $0.13R_{200}$.

The gas density profile steepen in the center with the age of the structure and b_3 varies from 0.3 to 1.1 in the hot system, from 0.4 to 1.2 in the cool one (Fig. 3). On the other hand, the outer

slope parameter, b_4 , when a single β - model is fitted (i.e. b_3 is fixed equals to zero) remains almost unchanged around values of 0.48 and 0.54 in the less and most massive object, respectively.

Single power-laws fitted between 0.01 and $0.1R_{200}$ and between 0.1 and $0.5R_{200}$, show a clear steepening in the surface brightness profiles, with the inner slope that smoothly changes with time from -0.6 to -1.2 (down to -1.4 in the cool system) and the outer slope, that varies mildly from -1.8 to -2 in the more massive cluster, and from -1.7 to -1.8 in the less massive system. When a single β -model is fitted the outer slope parameter, c_3 , is about 0.65 and 0.57 in the “8 keV” and “4 keV” object, respectively, for $r > 0.2R_{200}$, whereas decreases from 0.5 to 0.4 (cluster) and from 0.44 to 0.34 (group) when the joint-fit with the inner power-law is performed.

The logarithmic slope of the entropy profile α lies between 0.9 and 1.1 in the hot cluster and increases slightly from 0.6 to 1.1 in the cool system. The pedestal value K_0 show the largest variation, from about 270 (in the “8 keV” cluster; 100 in the “4 keV” one) keV cm^2 to zero in $\sim 7.5(2)$ Gyr (Fig. 3).

The slope γ of the cooling time profile remains approximately constant around 1.3 in the most massive system. It increases from 1.1 to 1.4 in the cool system with a corresponding decrease in the cooling time at $0.1R_{200}$ from 4 to 1 Gyr (see Fig. 3). The pedestal value t_0 is again the parameter more sensitive on the evolution of the central core, decreasing from 13.5 Gyr to zero in 9.5 Gyr in the

massive object, and from 8.5 Gyr to zero in 6 Gyr in the “4 keV” system.

Overall, the best-fit parameters that correlate more significantly with the age of the structure and the evolving cooling core are the inner slopes a_3 , b_3 , c_3 and the pedestal values K_0 and t_0 (see Fig. 3). For instance, under the action of the radiative cooling alone, we predict a variation by a factor of 3 in the inner slope of the gas density and surface brightness profile of massive systems and a corresponding steepening of the cooling time and entropy profiles within $0.1R_{200}$.

The cooling radius itself, R_{cool} , defined as the radius at which the cooling time equals the Universe age at given redshift, marks clearly the age of the structure subjected to radiative losses only, evolving from $\sim 0.01R_{200}$ at $z > 2$ to ~ 0.05 and $0.06R_{200}$ at $z = 0$ in the 8 and 4 keV system (panel at the bottom right in Fig. 3).

3.3 Comparison with observational constraints

The cool cores observed in nearby X-ray luminous galaxy clusters (e.g. Donahue et al. 2006, Sanderson et al. 2006, Dunn & Fabian 2008) show radial profiles well described by a single power-law with constant slope, like the inner temperature profile ($T_{\text{gas}} \propto r^{0.4}$), the cooling time profile ($t_{\text{cool}} \propto r^{1.3}$) and the entropy profile ($K \propto r^{1.1}$) outside the cooling region. All these slopes are well matched in our simple models (see, e.g., Fig. 3).

We compare our X-ray luminosity and emission weighted temperature estimates with the recent observational constraints obtained for a sample of 111 galaxy clusters in the redshift range $0.1 < z < 1.3$ with archived *Chandra* exposures in Maughan et al. (2007). We estimate “spectroscopic-like” temperature T_{sp} and luminosity both including and excluding the core emission within $0.15R_{500} \approx 0.1R_{200}$. The cool and the hot system behave similarly, with a luminosity from the core that rises with time from 25 up to 40 per cent of the total (within R_{500}) X-ray bolometric value, whereas the ratio between the emission weighted temperature in the core and within R_{500} decreases by about 35 per cent in 10 Gyrs. When the temperature and the luminosity are calculated within R_{500} , including the core region, the clusters evolve along wide trajectories in the $L - T$ plane (see dots in the right panel of Fig. 4). The value of the slope B of the $L - T$ relation remains constant around a value of 2.5, whereas the normalization $A = (L/10^{44} \text{ erg s}^{-1})/(T/5 \text{ keV})^B$ increases from 4.0 to 11.9 after 10 Gyrs. On the other hand, if, instead of the total cluster emission, we consider only the contribution from the region outside the core (i.e. $0.15R_{500} < r < R_{500}$), the luminosity and temperature estimates do not change significantly with the cosmic time, with a slope $B \sim 2.5$ and a normalization that rises by 17 per cent only in 10 Gyrs from the initial value $A = 3.4$. The predicted $L - T$ relation is compared in the left panel of Fig. 4 with the observational results obtained similarly from Maughan et al. (2007). By using a χ^2 minimization of a linear fit to the logarithmic values of the observed luminosity and temperature estimated for 111 clusters in the radial range $0.15R_{500} - R_{500}$, we measure a slope of 2.77 ± 0.08 , quite consistent with the range found in our simulated objects, and a normalization $A = 4.26 \pm 0.11$, that is just a factor 1.07–1.25 larger than our simulated relation calculated excluding the inner $0.15R_{500}$ at the present time.

In Fig. 4, the ratios between the gas temperature and luminosity estimated in $0.15 - 1R_{500}$ to those estimated in $0 - R_{500}$ are compared with the corresponding values estimated in the sample of Maughan et al. (2007). In particular, we associate an age

to each of the observed cluster, defined as the age of the models that minimizes the squared differences between the observed and predicted ratios $T_{\text{out}}/T_{\text{tot}} = T_{0.15-1R_{500}}/T_{0-1R_{500}}$ and $L_{\text{out}}/L_{\text{tot}} = L_{0.15-1R_{500}}/L_{0-1R_{500}}$, weighted by the propagated errors. Admittedly, this estimate for the age is very uncertain. An upper limit on the age is fixed equal to the age of the Universe at the object’s redshift minus one Gyr, to allow for the formation of the structure. We remind here that what we mean for “age” of the structure is something close, in the observational view of the cluster hierarchical formation, to the time elapsed since the last major merging able to affect the physical properties of the core, or even to destroy it. In other words, our “age” can be related to an “observational age” by the time during which a cluster evolves “passively”.

The data are then ordered by the estimated age, binned by 15–20 elements and plotted in the central panel of Fig. 4. Our rough estimates indicate that about 30 per cent of the clusters in the observed sample have an age less than 2 Gyr, 20 per cent are between 2 and 6 Gyrs old, the remaining 50 per cent is more than 6 Gyrs old, with 13 low-redshift objects with an age around 10 Gyrs. Moreover, the distribution of the age with respect to the median redshift ($z = 0.324$) indicates that the dynamically young structures (age < 6 Gyrs) are preferentially located at higher redshift (33 out of 54 objects), whereas about 60 per cent of clusters at lower redshift have an age higher than 6 Gyrs (35 out of 56 clusters). While the predicted ratio between the outer and total temperature ranges between 1 and 1.2 as actually observed, the contribution of the outer region to the total luminosity is expected from the models to be larger than 0.6 at any age, whereas the observed ratios reach values around 0.4. This ratio requires that the contribution in luminosity from the core with respect to the outer region should be twice than actually measured in our models (after 10 Gyrs, we estimate $L(< 0.15R_{500})/L(0.15 - 1R_{500}) \approx 0.7$, while a value ~ 1.5 would be required to match the observations), suggesting that more favourable conditions for cooling have to be provided (like different initial conditions; see next subsection) to generate objects with similar integrated properties.

3.4 Dependence of the profiles upon the initial conditions

The initial conditions described in section 2 are necessarily somewhat arbitrary. For our reference models, described above, we decided to use as initial temperature profiles at large radii the average profile observed by Vikhlinin et al. (2006). In the core region, instead, we considered isothermal gas. A different obvious choice would be to assume isothermal gas in the whole cluster (as in Brighenti & Mathews 2003 and Guo & Oh 2007). With this set-up, however, the observed negative temperature gradient for $r > 0.2R_{500}$ is not reproduced.

It is useful to compare how the results change if the ICM is assumed to be initially isothermal at every radius, with temperature calculated from the observed $M_{\text{tot}} - T$ relation by Arnaud et al. (2005). In this case, the central gas density required to have $f_b \sim 0.16$ at the virial radius is larger than in our reference models. This implies a correspondingly shorter cooling time (by $\sim 60\%$). As a consequence of that, our initially isothermal clusters age faster (the cooling catastrophe occurs earlier and reach a quasi steady-state sooner). At any given time, the cool cores are more developed than in the reference models, with a steeper density and surface brightness profiles with a ratio $n_{\text{gas}}(0.01R_{200})/n_{\text{gas}}(0.2R_{200})$ that reaches a value of 55 after 10 Gyr and the corresponding ratio in S_b more than a factor 2 larger than the reference value of ~ 60 (see Fig. 2).

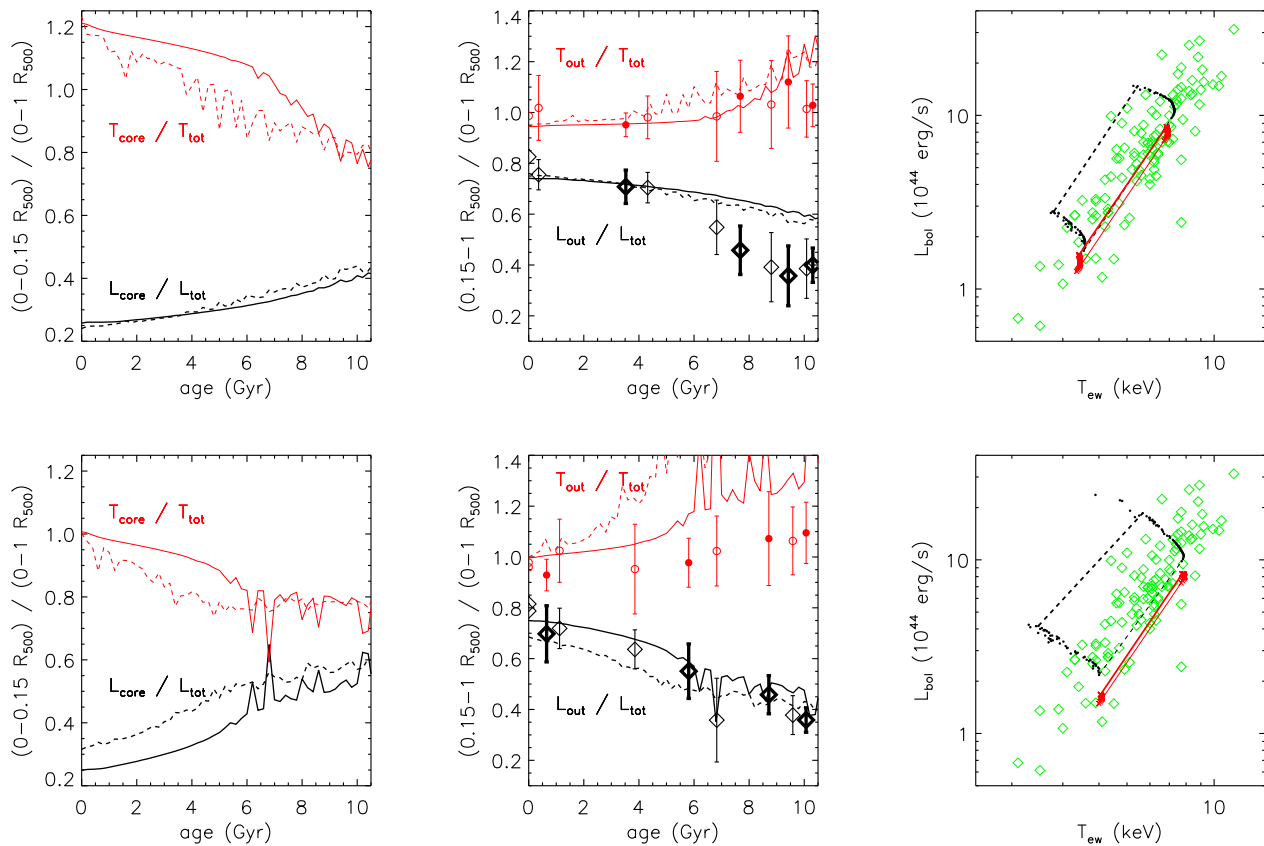


Figure 4. Evolution of the gas temperature and X-ray bolometric luminosity measurements. The **upper panels** refer to the reference model, whereas the **lower panels** adopt an isothermal profile as initial condition as described in Sect.3.4. (**Left**) Variation with the cosmic time of the core contribution to the total measurements for the “cool” system (*dashed lines*) and the “hot” cluster (*solid lines*). (**Middle**) Ratios between the values estimated at $0.15 - 1R_{500}$ and within R_{500} compared with the observational constraints in Maughan et al. (2007). The *thickest diamonds* represent the subsample of the most relaxed, less elliptical objects, selected with respect to the median values in centroid shifts and ellipticity measurements (see Table 2 in Maughan et al. 2007). The age of the observed clusters is defined as the age that minimizes the deviations between the observed and the predicted ratios in temperature and luminosity. (**Right**) Evolution in the $L - T$ diagram. We show estimates in the radial range $0.15 - 1R_{500}$ (*red crosses*) and within R_{500} without the exclusion of any core (*dots*). The lines connect the initial values (*thin line*) and the predicted ones after 10 Gyrs of evolution (*thick line*). The *green diamonds* represent the observed values in Maughan et al. (2007), when the core region $r < 0.15R_{500}$ is excised.

The relative contribution from the core to the total luminosity rises with the age of the core up to a value of 0.6, fifty per cent higher than maximum contribution observed in the reference models. Even the $L - T$ relation changes significantly as consequence of the larger emission from the core: when only the outer regions are considered (i.e. $0.15 - 1R_{500}$), the normalization A varies around 2.7, 60% lower than the observed value in the Maughan et al. (2007) sample (see Fig. 4).

We conclude that our results depend significantly upon the initial temperature profile chosen, if we maintain that gas fraction measured at the virial radius has to be consistent with the cosmological value. Once we adopt an initial temperature profile that well matches the observational constraints at $r > 0.15R_{500}$, we generate systems with a cool core in formation and not fully developed. The reason for this inconsistency is likely to be the non-evolution of the potential well in our models. Real massive clusters are still slowly growing with time (e.g. Li et al. 2007) and in their youth the ICM would have been cooler, with a shorter cooling time. This would contribute to develop a mature cool core sooner. To account the effects of an evolving potential well is beyond the goal of the present paper.

4 DISCUSSION AND CONCLUSIONS

We present a simple gasdynamic modelization of the X-ray emitting plasma in galaxy clusters subjected to the action of radiative processes only. These toy-models allow to follow and quantify the variations as function of the cosmic time of the physical quantities describing the cool cores in systems with a virial mass of $1.3 \times 10^{14} M_{\odot}$ and $1.3 \times 10^{15} M_{\odot}$, typical of a “4 keV” cluster and a “8 keV” cluster.

The cooling radius, R_{cool} , defined as the radius at which the cooling time equals the Universe age at given redshift, evolves from $\sim 0.01R_{200}$ at $z > 2$, where the structures begin their evolution, to $\sim 0.05(0.06)R_{200}$ at $z = 0$ in the 8 keV (4 keV) cluster (Fig. 3).

The temperature decreases with a mean rate around 10 per cent per Gyr when measured at $0.01R_{200}$, with the largest variation rate happening in the hot cluster when it is ~ 7 Gyr old with a decrement of the order of 15 per cent per Gyr. At the same time, the gas density and surface brightness increase with a rate of 15-20 per cent per Gyr at $0.01R_{200}$, reaching an incremental rate of 8 per cent per Gyr at the present time. As shown in the lower panels of Fig. 1, the systems reach a quasi-steady state. On the other hand,

the cool system has the largest variation at the beginning of its evolution (20 per cent in T_{gas} , 30 per cent in n_{gas} and S_b) and, then, varies slowly up to changes of few per cent after 10 Gyrs (Fig. 2). For pedagogical reasons, we run our models to a simulated age of 30 Gyr. Considering the state of still-developing cool cores, the variations in the future are quite significant, with a predicted rise of 78 (54) and 161 (126) per cent in n_{gas} and S_b , respectively, in the hot (cool) system and a decrease of 18 (10) per cent in T_{gas} at $0.01R_{200}$.

After 10 Gyr of radiative losses, the ratio between the gas temperature at $0.01R_{200}$, well within the cooling radius, and at $0.2R_{200}$, located beyond the cluster core, is equal to 0.4. The ratio between the gas densities at the same radii is ~ 35 , a factor $\sim 4 - 5$ larger than the ratio measured at the beginning of the formation of the cooling core. The surface brightness is observed to increase with the age of the structure with a mean rate of 20 and 2 per cent per Gyr at 0.01 and $0.2R_{200}$, respectively, implying a ratio that rises from 10 to ~ 60 at the present time in both of the objects.

The cooling time and gas entropy radial profiles are well represented by power-law functions, $t_{\text{cool}} = t_0 + t_{0.01}(r/0.01R_{200})^\gamma$ and $K = K_0 + K_{0.1}(r/0.1R_{200})^\alpha$, with t_0 and K_0 that decrease with time from 13.5 Gyrs and 270 keV cm^2 in the hot system (8.5 Gyr and 100 keV cm^2 in the cool one) and reaches zero after 9.5 (6) Gyrs. The slopes vary slightly with the age, with $\gamma \approx 1.3$ and $\alpha \approx 1.1$ (Fig. 3).

The behaviour of the inner slopes of the gas temperature and density profiles are the most sensitive and unambiguous tracers of an evolving cooling core. Their values after 10 Gyrs of radiative losses, $T_{\text{gas}} \propto r^{0.4}$ and $n_{\text{gas}} \propto r^{-1.1(-1.2)}$ for the hot (cool) object, are remarkably in agreement with the observational constraints available for nearby X-ray luminous cooling core clusters (e.g. Donahue et al. 2006, Sanderson et al. 2006, Dunn & Fabian 2008; see also the case of A1835 in Fig. 1). This implies that the heating process, if presently active, must not alter the ‘‘pure cooling flow’’ profiles in cool core clusters.

The emission-weighted temperature diminishes by about 25 per cent and the bolometric X-ray luminosity rises by ~ 60 per cent in 10 Gyrs when all the cluster emission is considered in the computation. On the contrary, when the core region within $0.15R_{500}$ is excluded, the gas temperature value does not vary and the X-ray luminosity changes by 20 per cent only. Observational constraints on the distribution of the $T(0.15 - 1R_{500})/T(< R_{500})$ as function of redshift (Maughan et al. 2007) show a mean value around 1 suggesting that the observed clusters cannot be significantly older than 8 Gyrs, once compared with the predictions from our models, independently from the initial conditions on the adopted temperature profile (see Fig. 4). As consequence of that, the value of the $L_{\text{out}}/L_{\text{tot}}$ ratio obtained in our model should be about 50 per cent lower to match the lower end of the observed distribution, implying a ratio between the core and the outer luminosities of ~ 1.5 , instead of the present predictions of about $0.4 - 0.7$ (see panel on the right in Fig. 4). More cooling at the core is therefore required to meet the observed trends. We show that this can be partially obtained by more flat temperature distribution in the outskirts, once the total gas fraction at the virial radius is fixed. Therefore, a tension between predicted and observed properties rises however when both the temperature profile and the temperature–luminosity relation have to be recovered consistently.

In this perspective, more detailed models following the energy distribution in the cluster outskirts in a cosmological context are required and matter for a following study.

ACKNOWLEDGMENTS

We acknowledge the financial contribution from contract ASI-INAF I/023/05/0 and I/088/06/0. We thank the anonymous referee for very useful comments that improved the presentation of the work.

REFERENCES

- Arnaud M., Pointecouteau E., Pratt G.W., 2005, *A&A*, 441, 893
 Bauer F.E., Fabian A.C., Sanders J.S., Allen S.W., Johnstone R.M., 2005, *MNRAS*, 359, 1481
 Brighenti F., Mathews W.G., 2000, *ApJ*, 535, 650
 Brighenti F., Mathews W.G., 2002, *ApJ*, 573, 542
 Brighenti F., Mathews W.G., 2003, *ApJ*, 587, 580
 Brighenti F., Mathews W.G., 2006, *ApJ*, 643, 120
 Bullock J.S., Kolatt T.S., Sigad Y., et al., 2001, *MNRAS*, 321, 559
 Donahue M., Horner D.J., Cavagnolo K.W., Voit G.M., 2006, *ApJ*, 643, 730
 Dunn R.J.H., Fabian A.C., 2008, *MNRAS*, in press (arXiv:0801.1215)
 Etti S., 2000, *MNRAS*, 318, 1041
 Etti S., Fabian A.C., Allen S.W., Johnstone R., 2002, *MNRAS*, 331, 635
 Etti S., Tozzi P., Borgani S., Rosati P., 2004, *A&A*, 417, 13
 Li Y., Mo H.J., van den Bosch F.C., Lin W.P., 2007, *MNRAS*, 379, 689
 Maughan B.J., Jones C., Jones L.R., Van Speybroeck L., 2007, *ApJ*, 659, 1125
 McNamara B., Nulsen P., 2007, *ARAA*, 45, 117
 Mellier Y., Mathez G., 1987, *A&A*, 175, 1
 Mohr J.J., Mathiesen B., Evrard A.E., 1999, *ApJ*, 517, 627
 Morandi A., Etti S., 2007, *MNRAS*, 380, 1521
 Navarro J.F., Frenk C.S., White S.D.M., 1996, *ApJ*, 462, 563
 Peterson J.R., Fabian A.C., 2006, *PhR*, 427, 1
 Salvador-Sol e E., Manrique A., Gonz alez-Casado G., Hansen S. H., 2007, *ApJ*, 666, 181 et al. 2007, *ApJ*, 666, 181
 Sanderson A.J.R., Ponman T.J., O’Sullivan E., 2006, *MNRAS*, 372, 1496
 Santos J.S., Rosati P., Tozzi P., Bhringer H., Etti S., Bignamini A., 2008, *A&A*, in press
 Shimizu M., Kitayama T., Sasaki S., Suto Y., 2003, *ApJ*, 590, 197
 Spergel D.N., Bean R., Dor e O., et al., 2007, *ApJS*, 170, 377
 Stone J.M., Norman M.L., 1992, *ApJS*, 80, 753
 Sutherland R.S., Dopita M.A., 1993, *ApJS*, 88, 253
 Vikhlinin A., Kravtsov A., Forman W., Jones C., Markevitch M., Murray S.S., Van Speybroeck L., 2006a, *ApJ*, 640, 691
 Vikhlinin A., Burenin R., Forman W.R., Jones C., Hornstrup A., Murray S.S., Quintana H., 2006b, Proceedings of ‘‘Heating vs. Cooling in Galaxies and Clusters of Galaxies’’, August 2006, Garching (Germany) (astro-ph/0611438)
 Zhao D.H., Mo H.J., Jing Y.P., B orner G., 2003, *MNRAS*, 339, 12